



**AIAA-2002-1659**

**Coupling Finite Element and Meshless Local  
Petrov-Galerkin Methods for Two-Dimensional  
Potential Problems**

T. Chen  
Army Research Laboratory  
NASA Langley Research Center  
Hampton, VA 23681

I.S. Raju  
NASA Langley Research Center  
Hampton, VA 23681

**43<sup>rd</sup> AIAA/ASME/ASCE/AHS/ASC  
Structures, Structural Dynamics, and  
Materials Conference  
22-25 April, 2002  
Denver, Colorado**



# COUPLING FINITE ELEMENT AND MESHLESS LOCAL PETROV-GALERKIN METHODS FOR TWO-DIMENSIONAL POTENTIAL PROBLEMS

T. Chen<sup>†</sup> and I.S. Raju<sup>\*</sup>

NASA Langley Research Center, Hampton, Virginia 23681-0001, USA

## Abstract

A coupled finite element (FE) method and meshless local Petrov-Galerkin (MLPG) method for analyzing two-dimensional potential problems is presented in this paper. The analysis domain is subdivided into two regions, a finite element (FE) region and a meshless (MM) region. A single weighted residual form is written for the entire domain. Independent trial and test functions are assumed in the FE and MM regions. A transition region is created between the two regions. The transition region blends the trial and test functions of the FE and MM regions. The trial function blending is achieved using a technique similar to the 'Coons patch' method that is widely used in computer-aided geometric design. The test function blending is achieved by using either FE or MM test functions on the nodes in the transition element.

The technique was evaluated by applying the coupled method to two potential problems governed by the Poisson equation. The coupled method passed all the patch test problems and gave accurate solutions for the problems studied.

**Keywords:** Finite element method, Meshless Local Petrov-Galerkin (MLPG), Coupling method, Potential problem

## Introduction

The finite element (FE) method [1, 2] is a widely used method, because of its accuracy, convenience, and flexibility. There are, however, deficiencies, such as element locking, discontinuous derivatives of the primary variable at element boundaries, and the need

for remeshing because of heavily distorted elements in large deformation. Meshless Methods (MM), such as the diffusion element method [3], the Element-Free Galerkin Method (EFGM) [4-6], h-p clouds [7], Partition of Unity (PU) [8], the Reproducing Kernel Particle Method (RKPM) [9], the Local Boundary Integral Equation (LBIE) method [10], and the Meshless Local Petrov-Galerkin (MLPG) method [11] are developed to avoid these deficiencies. Of these methods, the MLPG method is a very promising numerical method and has been successfully used on both potential and elasticity problems to obtain very accurate results [12-14]. The MLPG method is based on a local weak form and a moving least squares (MLS) approximation. This method is a "true" meshless method and does not need any "element" or "mesh" but uses a distributed set of nodes for both field interpolation and background integration. Although the MLPG method is attractive, the method is more computationally expensive than the FE method, and it is not as mature and comprehensive as the FE method.

There is a great interest in combining two different numerical methods, because such coupling would exploit the potential of each method while avoiding their deficiencies. Several techniques have been proposed in the literature [15-22] to couple different numerical methods, such as combining the FEM with the Boundary Element Method (BEM) [15, 16], the FEM with the EFGM [17, 20-22], the EFGM with the BEM [18], the FEM with the MLPG method [19], etc. In coupling methods, the analysis domain is divided into two regions and each method is used in a region where it is most efficient. At the interface between the regions, the continuity of the primary variable and the balance of the secondary variables need to be maintained. One technique that is commonly used in the coupling methods [15-19] defines a transition region between the two regions. In the transition region, a ramp transition function is chosen to combine the trial functions (shape functions) of the two numerical methods. This technique is straightforward and widely used in coupling different numerical methods. Using this technique, the continuity condition of the primary variable is satisfied. However, the reciprocity condition of the secondary variables is not guaranteed. Other

<sup>†</sup> Army Research Laboratory, MS-240, Analytical and Computational Methods Branch, NASA Langley Research Center.

<sup>\*</sup> Head, Analytical and Computational Methods Branch, Associate Fellow AIAA.

Copyright © 2002 by the American Institute of Aeronautics and Astronautics, Inc. No copyright is asserted in the United States under Title 17, U.S. Code. The U.S. Government has a royalty-free license to exercise all rights under the copyright claimed herein for Governmental Purposes. All other rights are reserved by the copyright owner.

techniques, such as Lagrange multipliers method [20], a hierarchical mixed approximation method [21], and a method that comprises both FE and EFGM shape functions in the interface region [22] have also been presented recently.

In this paper, a formulation that couples the FE and MLPG methods is presented for two-dimensional (2D) potential problems based on a single variational form. In this method, the analysis domain is divided into two regions (FEM region and MLPG region). Several computational issues related to the coupling method are discussed. Two numerical examples for the potential problems governed by Poisson equation are presented to evaluate the accuracy and efficiency of the proposed technique.

### Variational Coupling Procedure

In this section the variational coupling procedure is described for coupling two disjoint regions (sub-domains) that are governed by a potential function.

Consider a Poisson's equation for a 2D problem governing the potential  $u$  (primary variable) in a two-dimensional (2D) domain  $\Omega$  bounded by contour  $\Gamma$  (see Figure 1)

$$\nabla^2 u = p \quad (1)$$

The right hand side  $p$  in Eq. (1) is, in general, a function of  $x$  and  $y$ . In the general case, the boundary  $\Gamma$  can have mixed boundary conditions. On one part of the boundary,  $\Gamma_u$ , the potential  $u$  is prescribed, and on the remaining part  $\Gamma_q$ , the secondary variables, flux, ( $q = du/dn$ ) are prescribed, i. e.

$$u = \bar{u} \quad \text{on } \Gamma_u \quad \text{and} \quad q = \bar{q} \quad \text{on } \Gamma_q \quad (2)$$

where  $\Gamma = \Gamma_u \cup \Gamma_q$ . For example, in a steady-state heat transfer problem, which is a typical Poisson's problem,  $u$  is a temperature function,  $q$  is the heat flux function and  $p$  is internal heat generation.

The solution for Eq. (1) is sought in a weighted residual manner as

$$\int_{\Omega} \left( \frac{\partial^2 u}{\partial x^2} + \frac{\partial^2 u}{\partial y^2} - p \right) \cdot v \cdot dx \cdot dy = 0 \quad (3)$$

where  $v = v(x, y)$  is an arbitrary weight function.

Using the divergence theorem, one can rewrite Eq. (3) as

$$\begin{aligned} & - \int_{\Omega} \left( \frac{\partial u}{\partial x} \cdot \frac{\partial v}{\partial x} + \frac{\partial u}{\partial y} \cdot \frac{\partial v}{\partial y} \right) \cdot d\Omega + \int_{\Gamma} \left( \frac{\partial u}{\partial x} \cdot n_x + \frac{\partial u}{\partial y} \cdot n_y \right) \cdot v \cdot d\Gamma \\ & - \int_{\Omega} p \cdot v \cdot d\Omega = 0 \end{aligned} \quad (4)$$

where  $n_x$  and  $n_y$  are the direction cosines of the outward normal  $\mathbf{n}$  of the boundary in the  $x$  and  $y$  directions, respectively (see Figure 1).

In the coupling method, the domain  $\Omega$  is divided into an FE region ( $\Omega_F$ ) and an MM region ( $\Omega_M$ ) as shown in Figure 2. The subscripts F and M are used to describe the variables in the FE and MM regions, respectively. The interface between the two regions is denoted as  $\Gamma_I$ .

In the coupling method, the weighted residual equation (Eq. (3)) and subsequently the weak form (Eq. (4)) are written for the FE and MM regions separately as

$$\begin{aligned} I_F = & - \int_{\Omega_F} \left( \frac{\partial u}{\partial x} \cdot \frac{\partial v}{\partial x} + \frac{\partial u}{\partial y} \cdot \frac{\partial v}{\partial y} \right) \cdot d\Omega + \int_{\Gamma_F} \left( \frac{\partial u}{\partial x} \cdot n_x + \frac{\partial u}{\partial y} \cdot n_y \right) \cdot v \cdot d\Gamma \\ & + \int_{\Gamma_I} \left( \frac{\partial u}{\partial x} \cdot n_{Fx} + \frac{\partial u}{\partial y} \cdot n_{Fy} \right) \cdot v \cdot d\Gamma - \int_{\Omega_F} p \cdot v \cdot d\Omega = 0 \end{aligned} \quad (5)$$

$$\begin{aligned} I_M = & - \int_{\Omega_M} \left( \frac{\partial u}{\partial x} \cdot \frac{\partial v}{\partial x} + \frac{\partial u}{\partial y} \cdot \frac{\partial v}{\partial y} \right) \cdot d\Omega + \int_{\Gamma_M} \left( \frac{\partial u}{\partial x} \cdot n_x + \frac{\partial u}{\partial y} \cdot n_y \right) \cdot v \cdot d\Gamma \\ & + \int_{\Gamma_I} \left( \frac{\partial u}{\partial x} \cdot n_{Mx} + \frac{\partial u}{\partial y} \cdot n_{My} \right) \cdot v \cdot d\Gamma - \int_{\Omega_M} p \cdot v \cdot d\Omega = 0 \end{aligned} \quad (6)$$

Notice that the outward normals of interface boundary from FE and MM domains are in opposite directions (see Figure 2), i.e.

$$\mathbf{n}_F = -\mathbf{n}_M \quad (7)$$

Therefore, the terms along the interface boundary should meet the requirement

$$\begin{aligned} & \int_{\Gamma_I} \left( \frac{\partial u}{\partial x} \cdot n_{Fx} + \frac{\partial u}{\partial y} \cdot n_{Fy} \right) \cdot v \cdot d\Gamma \\ & + \int_{\Gamma_I} \left( \frac{\partial u}{\partial x} \cdot n_{Mx} + \frac{\partial u}{\partial y} \cdot n_{My} \right) \cdot v \cdot d\Gamma = 0 \end{aligned} \quad (8)$$

The balance of the secondary variables represented by Eq. (8) along the interface needs to be satisfied. This issue will be discussed in detail later in this paper.

Combing Eqs. (5) and (6) and using Eq. (8), a single variational equation that is valid for the entire domain  $\Omega$  can be written as

$$\begin{aligned} & - \int_{\Omega_{F'}} \left( \frac{\partial u}{\partial x} \cdot \frac{\partial v}{\partial x} + \frac{\partial u}{\partial y} \cdot \frac{\partial v}{\partial y} \right) \cdot d\Omega + \int_{\Gamma_{F'}} \left( \frac{\partial u}{\partial x} \cdot n_x + \frac{\partial u}{\partial y} \cdot n_y \right) \cdot v \cdot d\Gamma \\ & - \int_{\Omega_{F'}} p \cdot v \cdot d\Omega - \int_{\Omega_M} \left( \frac{\partial u}{\partial x} \cdot \frac{\partial v}{\partial x} + \frac{\partial u}{\partial y} \cdot \frac{\partial v}{\partial y} \right) \cdot d\Omega \\ & + \int_{\Gamma_M} \left( \frac{\partial u}{\partial x} \cdot n_x + \frac{\partial u}{\partial y} \cdot n_y \right) \cdot v \cdot d\Gamma - \int_{\Omega_M} p \cdot v \cdot d\Omega = 0 \end{aligned} \quad (9)$$

The next step in the coupling method is to choose the trial and test functions. The approximations for  $u$  in the variational form (Eq. (9)) are called the trial functions while the weight functions  $v$  in the variational form are called the test functions. The trial and test functions of the FE and MM methods along the interface ( $\Gamma_I$ ) are not the same. The coupling between the FE and MM regions can be achieved by defining a transition region  $\Omega_T$  (see in Figure 3.) The region  $\Omega_{F'}$  is split into two parts,  $\Omega_F$  and  $\Omega_T$ , with an interface  $\Gamma_T$ . The region  $\Omega_T$  is now between the FE region  $\Omega_F$  and the meshless region  $\Omega_M$ .

#### Trial and test functions

The trial and test functions for the FE and MM regions are presented first and then the functions in the transition region are discussed. The trial and test functions are chosen such that

$$u = u_F + u_M \text{ and } v = v_F + v_M \quad (10)$$

The trial functions of a point  $x$  in the FE region are

$$u_F = \begin{cases} \sum_{e=1}^{N_F} u_F^{(e)} & x \in \Omega_F \\ 0 & x \in \Omega_M \end{cases} \quad (11)$$

where  $u_F^{(e)}$  are the interpolation functions used in the traditional FE method, and  $N_F$  is the number of the elements in the FE region. Similarly, the trial functions in the MM region are

$$u_M = \begin{cases} 0 & x \in \Omega_F \\ \sum_{j=1}^{N_M} (u_M)_j & x \in \Omega_M \end{cases} \quad (12)$$

where  $N_M$  is the number of nodes in the MM region and  $(u_M)_j$  are the moving least squares (MLS) approximations at each of the nodes in the MM region. The test functions are chosen as

$$v_F = \begin{cases} \sum_{e=1}^{N_F} v_F^{(e)} & x \in \Omega_F \\ 0 & x \in \Omega_M \end{cases} \quad (13)$$

where  $v_F^{(e)}$  are chosen to be the variations on  $u_F^{(e)}$  (i.e.  $\delta u_F^{(e)}$ ) as is customary in the traditional FE method and

$$v_M = \begin{cases} 0 & x \in \Omega_F \\ \sum_{j=1}^{N_M} (v_M)_j & x \in \Omega_M \end{cases} \quad (14)$$

where  $(v_M)_j$  are chosen to be the Petrov-Galerkin weight function on a compact support sub-domain of each node [13]. The weight function of node  $i$  equals unity at  $x_i$ , and monotonically decreases as  $\|x - x_i\|$  increases and is equal to zero at the boundary and outside of the sub-domain.

#### Trial functions in the transition region

The trial functions in the transition region need special attention. Different numerical methods (MM, BEM, and different types of elements of FEM) use distinct trial functions. Directly coupling two numerical methods by only matching the interface nodal values may not satisfy the compatibility condition along the interface. In other words, the function values produced in different regions along the interface may be different although a few nodal values are the same. Therefore, a transition element between the two regions that smoothly transforms the values of the trial functions from one region to another is preferred.

A blending technique is developed to generate the interpolation function in a 4-sided region (quadrilateral element) in terms of its edge (boundary) functions (see Figure 4). The edges of the element can be curved and the number of the nodes on each of the edges need not be the same. This technique is similar to a technique, 'Coons patch' [23], that is used in computer-aided geometric design and FEM mesh generation. The Coons patch technique is used to construct a smooth surface using the bounded curves. By using the Coons patch technique in an analogous fashion, the various trial functions on the edges of the transition elements are blended smoothly. This technique is also similar to the method used to generate serendipity elements. However, instead of using the boundary nodal values to generate the serendipity element, the boundary functions are used in this blending technique to construct the transition element. These boundary functions may be explicit functions of the boundary nodal values, such as FEM, or implicit functions of the nodal values, such as MM.

A bilinear blending is used in this study to construct the trial function of the element. Although the blending is *bilinear*, the trial functions can be an *arbitrary* function that depends on the edge functions of the element [23]. To be compatible with the FE method, the trial functions of the transition element are developed in a square element (parent element) in the ' $\xi, \eta$ ' domain, where  $-1 \leq (\xi, \eta) \leq 1$ . The trial function can be written as

$$\begin{aligned}
 u = & \frac{1}{2}(1-\xi) \cdot \Gamma_3(\eta) + \frac{1}{2}(1+\xi) \cdot \Gamma_4(\eta) \\
 & + \frac{1}{2}(1-\eta) \cdot \Gamma_1(\xi) + \frac{1}{2}(1+\eta) \cdot \Gamma_2(\xi) \\
 & - \frac{1}{4}(1-\xi)(1-\eta) \cdot u_n - \frac{1}{4}(1+\xi)(1-\eta) \cdot u_p \\
 & - \frac{1}{4}(1+\xi)(1+\eta) \cdot u_q - \frac{1}{4}(1-\xi)(1+\eta) \cdot u_m
 \end{aligned} \quad (15)$$

where  $\Gamma_i$  ( $i = 1, 4$ ) are the boundary functions of the quadrilateral element and  $u_j$  ( $j = n, p, q$ , and  $m$ ) are the values of the primary variable at the corner nodes.

The derivatives of the primary variable with respect to  $x$  and  $y$  can be obtained by calculating the derivatives with respect to  $\xi$  and  $\eta$ , then forming the Jacobian matrix of the element and following standard FE procedures.

Typical transition elements between the FE region ( $\Omega_F$ ) and MM region ( $\Omega_M$ ) are shown in Figure 5. The open circles and solid circles represent the nodes in the FE and MM regions, respectively. The shaded elements are the transition elements. In these transition elements, the solid lines represent the boundaries that are connected to finite elements. On these boundaries, the edge functions can be generated by FE trial functions. The dashed lines in Figure 5 are the boundaries that connect to the MM region, and the edge functions are generated by the MM trial functions. The next step is to form the test function for the transition elements.

### Test functions in the transition region

Although the test function can be arbitrarily selected in the weighted residual method, to satisfy the weak form requirement of the reciprocity conditions of the secondary variables with constant derivatives (see Eq. (8)), the test functions  $v$  must (a) be the same function and (b) have the same integration length along the interface of both of the regions. Therefore, the test function of a node in the transition element depends on the adjacent regions of that node. If the node is adjacent only to the FE region, and not to the MM region, the FE test function is used and the integration length of the function is identical to the side of the element (for

example, the side lengths are  $a$  and  $b$  in type C of Figure 5 for node  $g$ ). For a node that connects to the MM region, the MM test function with a support domain of  $l_0$  is used (for example nodes  $q$  and  $k$  of type B in Figure 5).

One additional concern about the test function of the transition region is the size of the support domain of a node using an MM test function. The size of the support domain of an MM node can be defined by a process similar to that used in references [11-14]. Although there is no restriction on the size of the support domain by the weighted residual method, the radius ( $l_0$ ) of the support domain of a node is defined to be less than the size of the element to which that node belongs (see for example, nodes  $q$  and  $k$  of type B in Figure 5). This limitation on the size of the support domain eliminates complicated numerical integration that may be needed to integrate accurately the weak form of the transition element.

In Figure 5, three types of possible transition elements, A, B, and C, are identified. In the type B element, the nodes  $k$  and  $q$  are on the interface  $\Gamma_1$ . Therefore, the MM trial function is applied on edge  $kq$ , and the MM test functions should be applied on both nodes  $k$  and  $q$ . Note the sizes of the support domain ( $l_0$ ) of the test function for nodes  $k$  and  $q$  need not be the same. Since node  $q$  is shared by elements of type A and B, in order to satisfy the reciprocity conditions of the secondary variables on the common edge  $pq$ , the MM test function should be applied on node  $q$  of the element of type A, although no MM trial function is applied on any edge in element of type A.

### System equations

The trial and test functions outlined in Eqs. (10-15) are substituted into the weak form in Eq. (9) and the integrations are performed. This leads to a system of equations similar to the FE and MLPG methods

$$[\mathbf{K}] \cdot \{\mathbf{u}\} = \{\mathbf{f}\} \quad (16)$$

where  $[\mathbf{K}]$  contains the  $[\mathbf{K}_F]$ ,  $[\mathbf{K}_M]$  and  $[\mathbf{K}_T]$  matrices corresponding to the FE, MM and transition regions, respectively. Similarly,  $\{\mathbf{f}\}$  contains contributions from the three regions. The solution of the system of equations leads to the potentials  $\{\mathbf{u}\}$  at all the nodes in the model. Note that instead of working with fictitious nodal potentials  $\{\hat{\mathbf{u}}\}$  in the MM method the nodal potentials  $\{\mathbf{u}\}$  are used by making use of the procedures contained in reference [14].

### Boundary conditions

There are no special considerations necessary to apply essential boundary conditions on the model. However, the values of the natural boundary condition ('force')

depend on the type of nodes (FE or MM) on the transition element. Based on Eq.(4), the 'force' value on a node is calculated as

$$f_j = \int_{\Gamma_j} \left( \frac{\partial u}{\partial x} \cdot n_x + \frac{\partial u}{\partial y} \cdot n_y \right) \cdot v_j \cdot d\Gamma - \int_{\Omega_j} p \cdot v_j \cdot d\Omega \quad (17)$$

where  $v_j$  is the test function of the nodes  $j$ ,  $\Gamma_j$  is the boundary of the test function where the secondary variables, fluxes, are prescribed, and  $\Omega_j$  is the domain of the test function.

The formulation presented above for the coupled method is evaluated by performing patch test problems and by application to problems for which exact solutions are available.

### Numerical Examples

To evaluate the algorithm of coupling FE-MM for potential problems, two example problems governed by Poisson's equation, as shown in Figure 6, are considered. For the numerical integration in the MM domain, 8 and 12 Gauss points are used in the radial and tangential directions, respectively, of the circular support domain. A 3x3 quadrature rule is used for the quadratic elements in the FE region. The Gauss quadrature of a node in the transition element is dependent on the test function of the node. For the node using the MM test function, the same Gauss quadrature is used as in the MM region. A 4x4 quadrature rule is used for the node using the FE test functions.

The potential and its partial derivatives obtained using the coupling method are compared to exact solutions wherever available. The error norm ( $\|e_M\|_2$ ) is used to evaluate the effectiveness of various parameters. This norm is defined as

$$\|e_M\|_2 = \sqrt{\sum_{j=1}^M \left\{ (u_j - u_{exact}) / u_{exact} \right\}^2} / M \quad (18)$$

where  $M$  is the total number of randomly distributed internal points in the domain at which the numerical solution is evaluated and compared to the exact solution. Note that these internal points are independent points that are randomly generated and are not associated with the nodes used in the models. In the MM region, a value of  $M = 50$  is used, and in the FE region, six randomly distributed points are generated for each element. The error norm is calculated for the entire domain. If the exact solution of the problem is not available, the results of the coupling method are compared to the full FE solutions and the full MM solutions over the analysis domain.

Two types of interfaces are used to model the examples. The first type of interface cuts across the domain and intersects the domain boundary as shown in Figure 2(a).

The second type of interface forms a closed loop and does not intersect the domain boundary (see Figure 2(b)). Two types of models are used to evaluate this type of interface. The first model uses an FE region that is embedded in an MM region, and the second model uses an MM region that is embedded in an FE region.

In the examples (see Figure 6), 8-node quadratic isoparametric elements and quadratic basis functions in the MM region are used. When the coupled method reproduces the exact solution, then the method "passes" the patch tests.

### Example 1

A potential problem governed by the Poisson's equation,  $\nabla u^2 = 2 \cdot (c_1 + c_2)$  is considered in a rectangular domain (Figure 6(a)). The exact solution for the problem is  $u = c_1 x^2 + c_2 y^2 + c_3 xy$ , where  $c_i$  are arbitrary constants. All four models in Figure 7 are used to evaluate the coupling method using quadratic quadrilateral elements and a quadratic basis function in the FE and MM regions, respectively. A type-I interface is used in the first model, and a type-II interface is used in the models 2, 3 and 4. In these patch tests, the potential  $u$  is prescribed on the boundaries of the entire domain corresponding to the exact values. As expected, the exact solutions for both potential and fluxes in the entire domain are reproduced to machine accuracy. Similar results are obtained using the mixed boundary conditions.

### Example 2

The second example considered is that of the torsion of a shaft of elliptical cross-section as shown in Figure 6(b). The governing equation is a Poisson's equation in terms of Prandtl stress function  $u$  with the boundary condition  $u = 0$  on the boundary of the cross-section. The shear stresses in the shaft are determined as the derivatives of the stress function. For this problem, the right-hand side function of Eq. (1) is defined as

$$p(x, y) = -2G\theta = -\frac{2 \cdot M \cdot (a^2 + b^2)}{\pi \cdot a^3 \cdot b^3} \quad (19)$$

where  $G$  is the modulus of rigidity,  $\theta$  is the twist angle,  $M$  is the torsion moment applied on the shaft, and  $a$  and  $b$  are the semi-major and semi-minor axes of the elliptic cross-section, respectively. The exact solution of the problem [24] is

$$u(x, y) = -\frac{M}{\pi \cdot a \cdot b} \left( \frac{x^2}{a^2} + \frac{y^2}{b^2} - 1 \right) \quad (20)$$

Two coupling models are used for the problem, a full model of the elliptic shaft and a model of one-quarter of the shaft, as shown in Figure 8. As the exact solution is a quadratic, quadratic elements and quadratic basis

functions are used. In the full model, 16 quadratic elements (8-node quadrilateral) and 102 MM nodes using a quadratic basis function are used. The essential boundary condition of  $u = 0$  is applied on the outer surface of the elliptic cross-section. In the model of one-quarter of the elliptic shaft, 4 quadratic elements and 38 nodes are used. The essential boundary condition ( $u = 0$ ) is applied on the outer surface and the natural boundary conditions ( $q = 0$ ) are applied on the symmetric centerlines ( $y = 0$  and  $x = 0$ ).

The error norm of the results for the potential and its first derivatives are computed using the exact solution at 100 randomly distributed points in the MM region and 96 random points in the FE region for the whole model. For the model of one-quarter of the elliptic shaft, 50 and 24 points are used in the MM and FE regions, respectively. The exact solutions are reproduced to machine accuracy for both models.

### Concluding Remarks

A technique is presented for coupling the traditional finite element (FE) method and the meshless method (MM) for analyzing two-dimensional potential problems that are governed by Poisson's equation. The coupling method allows the domain to be analyzed by the FE method in one region and the MM in another region. The regions are chosen depending on where each of methods is most effective.

A single variational weighted residual formulation is used on the entire domain to develop the coupling method. A transition region is defined between the FE region and the MM region. In the transition region, a blending technique is used to construct the trial function based on the trial function in the adjacent region. The MM and FE test functions are used in the transition region to satisfy the compatibility condition of the secondary variables.

Potential patch test problems involving Poisson equation are used to evaluate the effectiveness of the coupling technique when the meshless local Petrov-Galerkin method is used in the MM region. The coupling method passed all the patch test problems and yielded very accurate solutions for the problems studied.

### References

- [1] Zienkiewicz, O.C., and Taylor, R.L., *The Finite Element Method*, 4th ed, McGraw-Hill Book Company, 1989.
- [2] Cook, R.D., Malkus, D.S., and Plesha, M.E., *Concepts and Applications of Finite Element Analysis*, 3rd ed, John Wiley and Sons, 1989.
- [3] Nayroles, B., Touzot, G., and Villon, P., "Generalizing the Finite Element Method: Diffuse Approximation and Diffuse Elements," *Computational Mechanics*, Vol. 10, No. 5, 1992, pp. 307-318.
- [4] Belytschko, T., Lu, Y.Y., and Gu, L., "Element-Free Galerkin Methods," *International Journal for Numerical Methods in Engineering*, Vol. 37, No. 2, 1994, pp. 229-256.
- [5] Belytschko, T., Lu, Y.Y., and Gu, L., "Crack Propagation by Element-Free Galerkin Methods," *Engineering Fracture Mechanics*, Vol. 51, No. 2, 1995, pp. 295-315.
- [6] Lu, Y.Y., Belytschko, T., and Gu, L., "New Implementation of the Element Free Galerkin Method," *Computer Methods in Applied Mechanics and Engineering*, Vol. 113, No. 3-4, 1994, pp. 397-414.
- [7] Duarte, C., and Oden, J.T., "Hp Clouds - an Hp Meshless Method," *Numerical Methods for Partial Differential Equations*, Vol. 12, 1996, pp. 673-705.
- [8] Melenk, J.M., and Babuska, I., "The Partition of Unity Finite Element Method: Basic Theory and Applications," *Computer Methods in Applied Mechanics and Engineering*, Vol. 139, 1996, pp. 289-314.
- [9] Liu, W.K., Jun, S., and Zhang, Y.F., "Reproducing Kernel Particle Methods," *International Journal for Numerical Methods in Engineering*, Vol. 20, 1995, pp. 1081-1106.
- [10] Zhu, T., Zhang, J.D., and Atluri, S.N., "A Local Boundary Integral Equation (LBIE) Method in Computational Mechanics, and a Meshless Discretization Approach," *Computational Mechanics*, Vol. 21, No. 3, 1998, pp. 223-235.
- [11] Atluri, S.N., and Zhu, T., "A New Meshless Local Petrov-Galerkin (MLPG) Approach in Computational Mechanics," *Computational Mechanics*, Vol. 22, No. 2, 1998, pp. 117-127.
- [12] Atluri, S.N., and Zhu, T.L., "Meshless Local Petrov-Galerkin (MLPG) Approach for Solving Problems in Elasto-Statics," *Computational Mechanics*, Vol. 25, No. 2, 2000, pp. 169-179.
- [13] Raju, I.S., and Chen, T., "Meshless Petrov-Galerkin Method Applied to Axisymmetric Problems," Proceedings of the 42nd AIAA/ASME/ASCE/AHS/ASC Structures, Structural Dynamics, and Materials Conference, Seattle, Washington, April 16-19, 2001.



- [14] Atluri, S.N., Kim, H.-G., and Cho, J.Y., "A Critical Assessment of the Truly Meshless Local Petrov-Galerkin (MLPG), and Local Boundary Integral Equation (LBIE) Methods," *Computational Mechanics*, Vol. 24, No. 5, 1999, pp. 348-372.
- [15] Zienkiewicz, O.C., Kelly, D.W., and Bettress, F., "The Coupling of the Finite Element Method and Boundary Solution Procedures," *International Journal for Numerical Methods in Engineering*, Vol. 11, 1977, pp. 355-375.
- [16] Krishnamurthy, T., and Raju, I.S., "Coupling Finite and Boundary Element Methods for Two-Dimensional Potential Problems," *International Journal for Numerical Methods in Engineering*, Vol. 36, 1993, pp. 3593-3616.
- [17] Belytschko, T., Organ, D., and Krongauz, Y., "Coupled Finite Element-Element-Free Galerkin Method," *Computational Mechanics*, Vol. 17, No. 3, 1995, pp. 186-195.
- [18] Liu, G.R., and Gu, Y.T., "Coupling of Element Free Galerkin and Hybrid Boundary Element Methods Using Modified Variational Formulation," *Computational Mechanics*, Vol. 26, No. 2, 2000, pp. 166-173.
- [19] Liu, G.R., and Gu, Y.T., "Meshless Local Petrov-Galerkin (MLPG) Method in Combination with Finite Element and Boundary Element Approaches," *Computational Mechanics*, Vol. 26, No. 6, 2000, pp. 536-546.
- [20] Hegen, D., "Element-Free Galerkin Methods in Combination with Finite Element Approaches," *Computer Methods in Applied Mechanics and Engineering*, Vol. 135, No. 1-2, 1996, pp. 143-166.
- [21] Huerta, A., and Fernandez-Mendez, S., "Enrichment and Coupling of the Finite Element and Meshless Methods," *International Journal for Numerical Methods in Engineering*, Vol. 48, No. 11, 2000, pp. 1615-1636.
- [22] Rao, B.N., and Rahman, S., "A Coupled Meshless-Finite Element Method for Fracture Analysis of Cracks," *International Journal of Pressure Vessels and Piping*, Vol. 78, No. 9, 2001, pp. 647-657.
- [23] Coons, S.A., "Surfaces for Computer-Aided Design of Space Forms," MIT, MAC - TR - 41, Cambridge, Mass., 1967.
- [24] Timoshenko, S.P., and Goodier, J.N., *Theory of Elasticity*, 3rd ed, McGraw-Hill, New York, 1965.

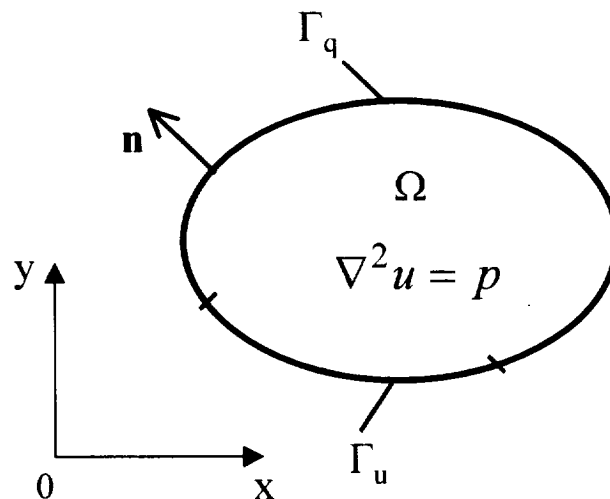


**Figure 1** Two-dimensional potential problem

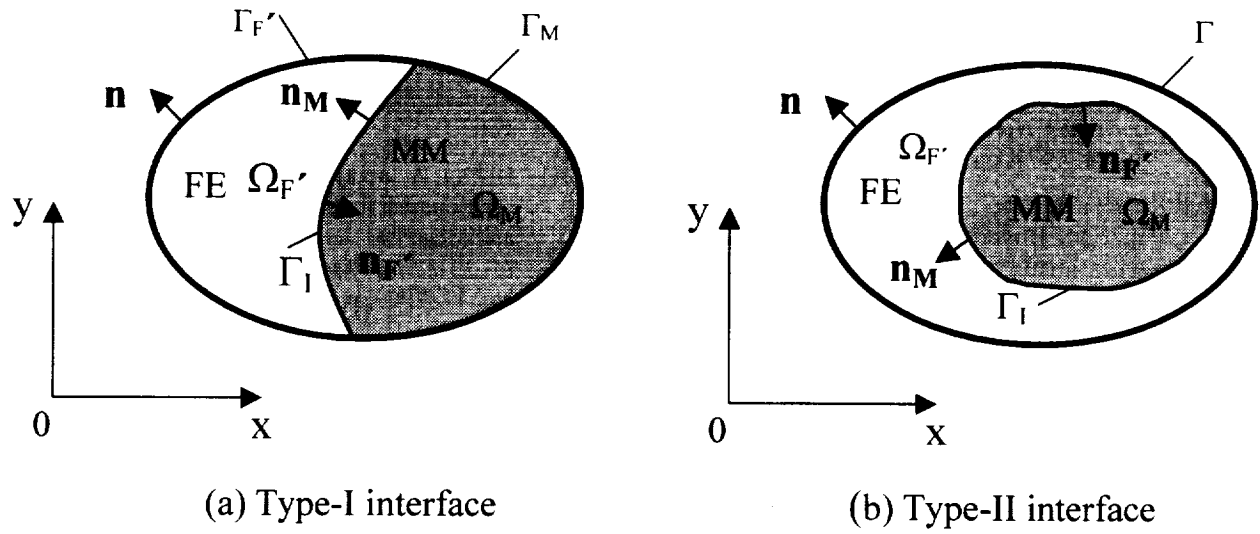


**Figure 2** Finite element and meshless method regions

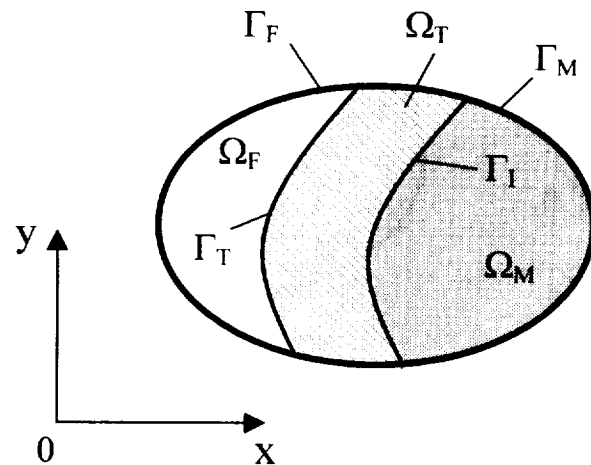


**Figure 3** Finite element (FE) region, transition (TR) region and meshless method (MM) region

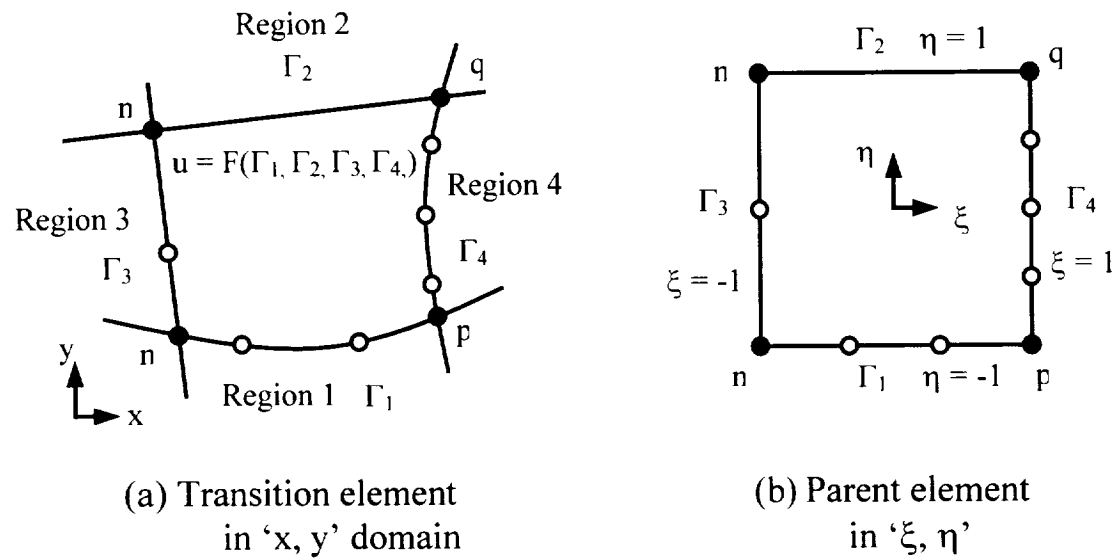


**Figure 4** Construction of transition element

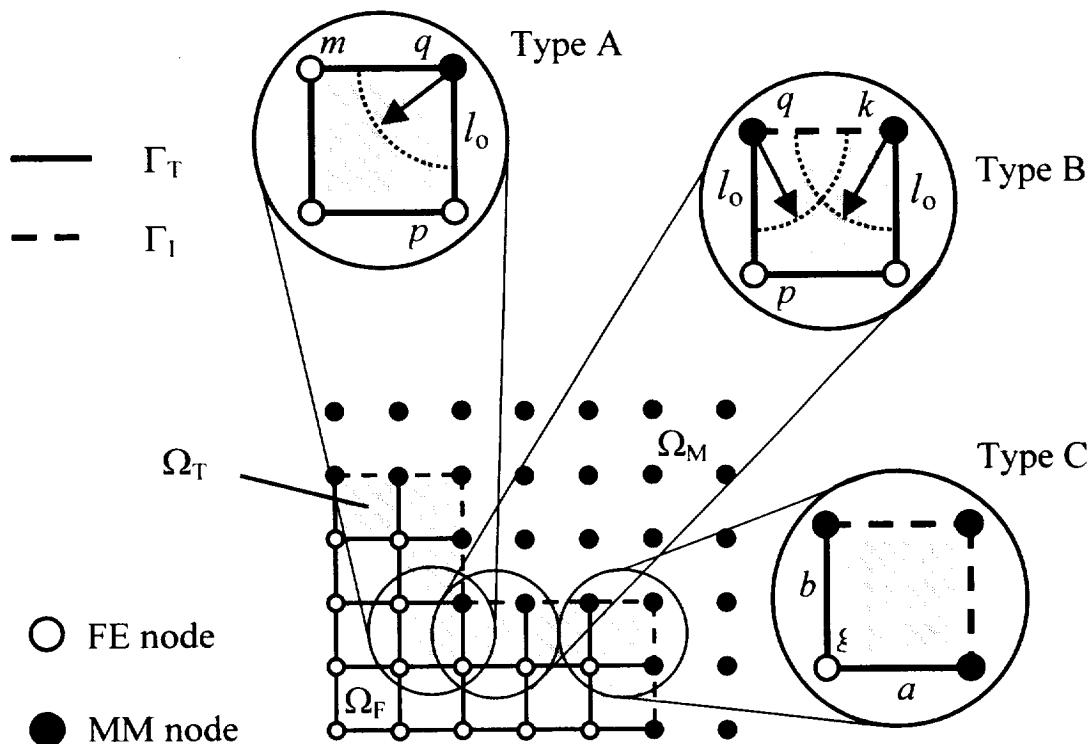
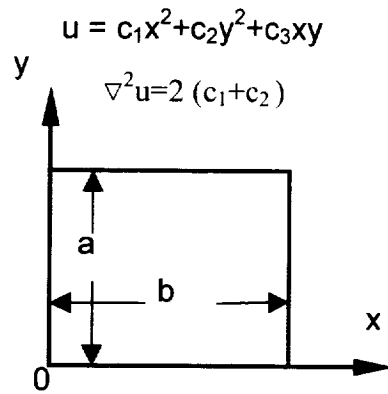
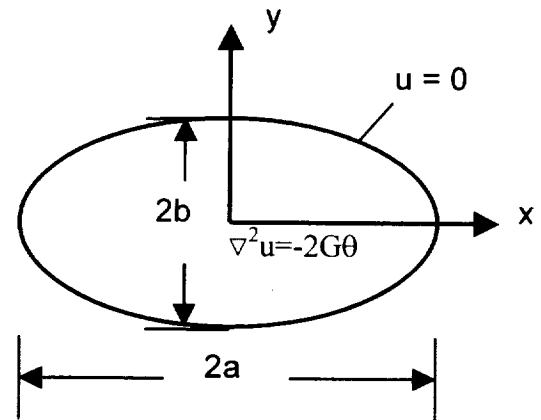


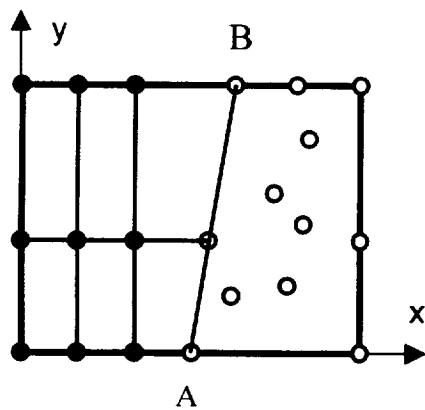
**Figure 5** Typical transition elements



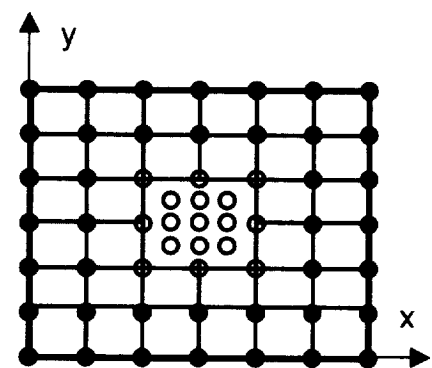
(a) Example - 1



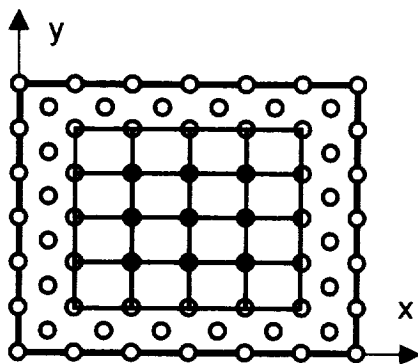
(b) Example - 2

**Figure 6** Examples governed by Poisson's equation

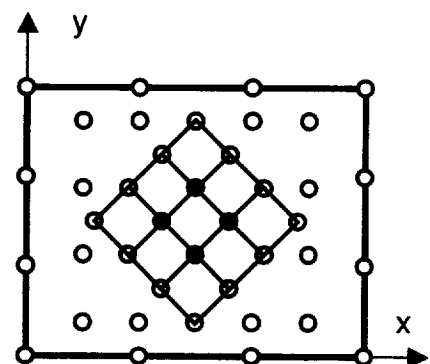
(a) Model 1



(b) Model 2

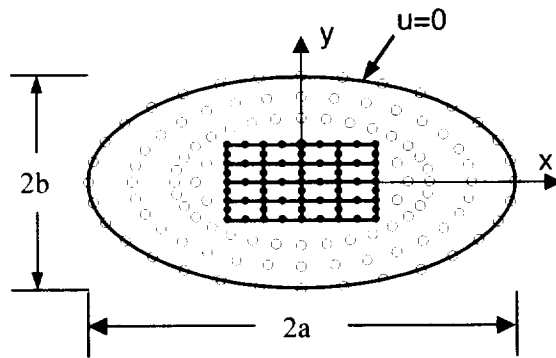


(c) Model 3

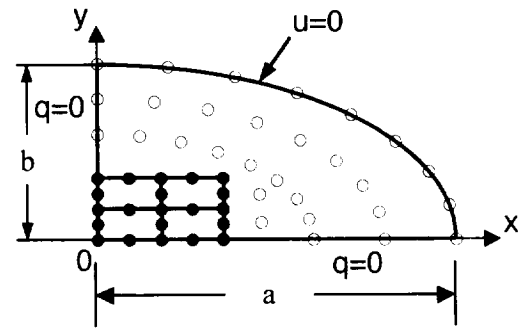


(d) Model 4

**Figure 7** Models used in the patch tests



(a) Whole elliptic shaft model



(b) Model of one-quarter of elliptic shaft

**Figure 8** Coupling models used in the elliptic shaft in torsion





**AIAA-2002-1659**

**Coupling Finite Element and Meshless Local  
Petrov-Galerkin Methods for Two-Dimensional  
Potential Problems**

T. Chen  
Army Research Laboratory  
NASA Langley Research Center  
Hampton, VA 23681

I.S. Raju  
NASA Langley Research Center  
Hampton, VA 23681

**43<sup>rd</sup> AIAA/ASME/ASCE/AHS/ASC  
Structures, Structural Dynamics, and  
Materials Conference  
22-25 April, 2002  
Denver, Colorado**





# COUPLING FINITE ELEMENT AND MESHLESS LOCAL PETROV-GALERKIN METHODS FOR TWO-DIMENSIONAL POTENTIAL PROBLEMS

T. Chen<sup>†</sup> and I.S. Raju<sup>\*</sup>

NASA Langley Research Center, Hampton, Virginia 23681-0001, USA

## Abstract

A coupled finite element (FE) method and meshless local Petrov-Galerkin (MLPG) method for analyzing two-dimensional potential problems is presented in this paper. The analysis domain is subdivided into two regions, a finite element (FE) region and a meshless (MM) region. A single weighted residual form is written for the entire domain. Independent trial and test functions are assumed in the FE and MM regions. A transition region is created between the two regions. The transition region blends the trial and test functions of the FE and MM regions. The trial function blending is achieved using a technique similar to the 'Coons patch' method that is widely used in computer-aided geometric design. The test function blending is achieved by using either FE or MM test functions on the nodes in the transition element.

The technique was evaluated by applying the coupled method to two potential problems governed by the Poisson equation. The coupled method passed all the patch test problems and gave accurate solutions for the problems studied.

**Keywords:** Finite element method, Meshless Local Petrov-Galerkin (MLPG), Coupling method, Potential problem

## Introduction

The finite element (FE) method [1, 2] is a widely used method, because of its accuracy, convenience, and flexibility. There are, however, deficiencies, such as element locking, discontinuous derivatives of the primary variable at element boundaries, and the need

for remeshing because of heavily distorted elements in large deformation. Meshless Methods (MM), such as the diffusion element method [3], the Element-Free Galerkin Method (EFGM) [4-6], h-p clouds [7], Partition of Unity (PU) [8], the Reproducing Kernel Particle Method (RKPM) [9], the Local Boundary Integral Equation (LBIE) method [10], and the Meshless Local Petrov-Galerkin (MLPG) method [11] are developed to avoid these deficiencies. Of these methods, the MLPG method is a very promising numerical method and has been successfully used on both potential and elasticity problems to obtain very accurate results [12-14]. The MLPG method is based on a local weak form and a moving least squares (MLS) approximation. This method is a "true" meshless method and does not need any "element" or "mesh" but uses a distributed set of nodes for both field interpolation and background integration. Although the MLPG method is attractive, the method is more computationally expensive than the FE method, and it is not as mature and comprehensive as the FE method.

There is a great interest in combining two different numerical methods, because such coupling would exploit the potential of each method while avoiding their deficiencies. Several techniques have been proposed in the literature [15-22] to couple different numerical methods, such as combining the FEM with the Boundary Element Method (BEM) [15, 16], the FEM with the EFGM [17, 20-22], the EFGM with the BEM [18], the FEM with the MLPG method [19], etc. In coupling methods, the analysis domain is divided into two regions and each method is used in a region where it is most efficient. At the interface between the regions, the continuity of the primary variable and the balance of the secondary variables need to be maintained. One technique that is commonly used in the coupling methods [15-19] defines a transition region between the two regions. In the transition region, a ramp transition function is chosen to combine the trial functions (shape functions) of the two numerical methods. This technique is straightforward and widely used in coupling different numerical methods. Using this technique, the continuity condition of the primary variable is satisfied. However, the reciprocity condition of the secondary variables is not guaranteed. Other

<sup>†</sup> Army Research Laboratory, MS-240, Analytical and Computational Methods Branch, NASA Langley Research Center.

<sup>\*</sup> Head, Analytical and Computational Methods Branch, Associate Fellow AIAA.

Copyright © 2002 by the American Institute of Aeronautics and Astronautics, Inc. No copyright is asserted in the United States under Title 17, U.S. Code. The U.S. Government has a royalty-free license to exercise all rights under the copyright claimed herein for Governmental Purposes. All other rights are reserved by the copyright owner.

techniques, such as Lagrange multipliers method [20], a hierarchical mixed approximation method [21], and a method that comprises both FE and EFGM shape functions in the interface region [22] have also been presented recently.

In this paper, a formulation that couples the FE and MLPG methods is presented for two-dimensional (2D) potential problems based on a single variational form. In this method, the analysis domain is divided into two regions (FEM region and MLPG region). Several computational issues related to the coupling method are discussed. Two numerical examples for the potential problems governed by Poisson equation are presented to evaluate the accuracy and efficiency of the proposed technique.

### Variational Coupling Procedure

In this section the variational coupling procedure is described for coupling two disjoint regions (sub-domains) that are governed by a potential function.

Consider a Poisson's equation for a 2D problem governing the potential  $u$  (primary variable) in a two-dimensional (2D) domain  $\Omega$  bounded by contour  $\Gamma$  (see Figure 1)

$$\nabla^2 u = p \quad (1)$$

The right hand side  $p$  in Eq. (1) is, in general, a function of  $x$  and  $y$ . In the general case, the boundary  $\Gamma$  can have mixed boundary conditions. On one part of the boundary,  $\Gamma_u$ , the potential  $u$  is prescribed, and on the remaining part  $\Gamma_q$ , the secondary variables, flux, ( $q = du/dn$ ) are prescribed, *i. e.*

$$u = \bar{u} \quad \text{on } \Gamma_u \quad \text{and} \quad q = \bar{q} \quad \text{on } \Gamma_q \quad (2)$$

where  $\Gamma = \Gamma_u \cup \Gamma_q$ . For example, in a steady-state heat transfer problem, which is a typical Poisson's problem,  $u$  is a temperature function,  $q$  is the heat flux function and  $p$  is internal heat generation.

The solution for Eq. (1) is sought in a weighted residual manner as

$$\int_{\Omega} \left( \frac{\partial^2 u}{\partial x^2} + \frac{\partial^2 u}{\partial y^2} - p \right) \cdot v \cdot dx \cdot dy = 0 \quad (3)$$

where  $v = v(x, y)$  is an arbitrary weight function.

Using the divergence theorem, one can rewrite Eq. (3) as

$$\begin{aligned} & - \int_{\Omega} \left( \frac{\partial u}{\partial x} \cdot \frac{\partial v}{\partial x} + \frac{\partial u}{\partial y} \cdot \frac{\partial v}{\partial y} \right) \cdot d\Omega + \int_{\Gamma} \left( \frac{\partial u}{\partial x} \cdot n_x + \frac{\partial u}{\partial y} \cdot n_y \right) \cdot v \cdot d\Gamma \\ & - \int_{\Omega} p \cdot v \cdot d\Omega = 0 \end{aligned} \quad (4)$$

where  $n_x$  and  $n_y$  are the direction cosines of the outward normal  $\mathbf{n}$  of the boundary in the  $x$  and  $y$  directions, respectively (see Figure 1).

In the coupling method, the domain  $\Omega$  is divided into an FE region ( $\Omega_F$ ) and an MM region ( $\Omega_M$ ) as shown in Figure 2. The subscripts F and M are used to describe the variables in the FE and MM regions, respectively. The interface between the two regions is denoted as  $\Gamma_I$ .

In the coupling method, the weighted residual equation (Eq. (3)) and subsequently the weak form (Eq. (4)) are written for the FE and MM regions separately as

$$\begin{aligned} I_F = & - \int_{\Omega_F} \left( \frac{\partial u}{\partial x} \cdot \frac{\partial v}{\partial x} + \frac{\partial u}{\partial y} \cdot \frac{\partial v}{\partial y} \right) \cdot d\Omega + \int_{\Gamma_F} \left( \frac{\partial u}{\partial x} \cdot n_x + \frac{\partial u}{\partial y} \cdot n_y \right) \cdot v \cdot d\Gamma \\ & + \int_{\Gamma_I} \left( \frac{\partial u}{\partial x} \cdot n_{Fx} + \frac{\partial u}{\partial y} \cdot n_{Fy} \right) \cdot v \cdot d\Gamma - \int_{\Omega_F} p \cdot v \cdot d\Omega = 0 \end{aligned} \quad (5)$$

$$\begin{aligned} I_M = & - \int_{\Omega_M} \left( \frac{\partial u}{\partial x} \cdot \frac{\partial v}{\partial x} + \frac{\partial u}{\partial y} \cdot \frac{\partial v}{\partial y} \right) \cdot d\Omega + \int_{\Gamma_M} \left( \frac{\partial u}{\partial x} \cdot n_x + \frac{\partial u}{\partial y} \cdot n_y \right) \cdot v \cdot d\Gamma \\ & + \int_{\Gamma_I} \left( \frac{\partial u}{\partial x} \cdot n_{Mx} + \frac{\partial u}{\partial y} \cdot n_{My} \right) \cdot v \cdot d\Gamma - \int_{\Omega_M} p \cdot v \cdot d\Omega = 0 \end{aligned} \quad (6)$$

Notice that the outward normals of interface boundary from FE and MM domains are in opposite directions (see Figure 2), *i. e.*

$$\mathbf{n}_F = -\mathbf{n}_M \quad (7)$$

Therefore, the terms along the interface boundary should meet the requirement

$$\begin{aligned} & \int_{\Gamma_I} \left( \frac{\partial u}{\partial x} \cdot n_{Fx} + \frac{\partial u}{\partial y} \cdot n_{Fy} \right) \cdot v \cdot d\Gamma \\ & + \int_{\Gamma_I} \left( \frac{\partial u}{\partial x} \cdot n_{Mx} + \frac{\partial u}{\partial y} \cdot n_{My} \right) \cdot v \cdot d\Gamma = 0 \end{aligned} \quad (8)$$

The balance of the secondary variables represented by Eq. (8) along the interface needs to be satisfied. This issue will be discussed in detail later in this paper.

Combing Eqs. (5) and (6) and using Eq. (8), a single variational equation that is valid for the entire domain  $\Omega$  can be written as

$$\begin{aligned} & - \int_{\Omega_F} \left( \frac{\partial u}{\partial x} \cdot \frac{\partial v}{\partial x} + \frac{\partial u}{\partial y} \cdot \frac{\partial v}{\partial y} \right) \cdot d\Omega + \int_{\Gamma_F} \left( \frac{\partial u}{\partial x} \cdot n_x + \frac{\partial u}{\partial y} \cdot n_y \right) \cdot v \cdot d\Gamma \\ & - \int_{\Omega_F} p \cdot v \cdot d\Omega - \int_{\Omega_M} \left( \frac{\partial u}{\partial x} \cdot \frac{\partial v}{\partial x} + \frac{\partial u}{\partial y} \cdot \frac{\partial v}{\partial y} \right) \cdot d\Omega \\ & + \int_{\Gamma_M} \left( \frac{\partial u}{\partial x} \cdot n_x + \frac{\partial u}{\partial y} \cdot n_y \right) \cdot v \cdot d\Gamma - \int_{\Omega_M} p \cdot v \cdot d\Omega = 0 \end{aligned} \quad (9)$$

The next step in the coupling method is to choose the trial and test functions. The approximations for  $u$  in the variational form (Eq. (9)) are called the trial functions while the weight functions  $v$  in the variational form are called the test functions. The trial and test functions of the FE and MM methods along the interface ( $\Gamma_I$ ) are not the same. The coupling between the FE and MM regions can be achieved by defining a transition region  $\Omega_T$  (see in Figure 3.) The region  $\Omega_F$  is split into two parts,  $\Omega_F$  and  $\Omega_T$ , with an interface  $\Gamma_T$ . The region  $\Omega_T$  is now between the FE region  $\Omega_F$  and the meshless region  $\Omega_M$ .

#### Trial and test functions

The trial and test functions for the FE and MM regions are presented first and then the functions in the transition region are discussed. The trial and test functions are chosen such that

$$u = u_F + u_M \text{ and } v = v_F + v_M \quad (10)$$

The trial functions of a point  $x$  in the FE region are

$$u_F = \begin{cases} \sum_{e=1}^{N_F} u_F^{(e)} & x \in \Omega_F \\ 0 & x \in \Omega_M \end{cases} \quad (11)$$

where  $u_F^{(e)}$  are the interpolation functions used in the traditional FE method, and  $N_F$  is the number of the elements in the FE region. Similarly, the trial functions in the MM region are

$$u_M = \begin{cases} 0 & x \in \Omega_F \\ \sum_{j=1}^{N_M} (u_M)_j & x \in \Omega_M \end{cases} \quad (12)$$

where  $N_M$  is the number of nodes in the MM region and  $(u_M)_j$  are the moving least squares (MLS) approximations at each of the nodes in the MM region. The test functions are chosen as

$$v_F = \begin{cases} \sum_{e=1}^{N_F} v_F^{(e)} & x \in \Omega_F \\ 0 & x \in \Omega_M \end{cases} \quad (13)$$

where  $v_F^{(e)}$  are chosen to be the variations on  $u_F^{(e)}$  (i.e.  $\delta u_F^{(e)}$ ) as is customary in the traditional FE method and

$$v_M = \begin{cases} 0 & x \in \Omega_F \\ \sum_{j=1}^{N_M} (v_M)_j & x \in \Omega_M \end{cases} \quad (14)$$

where  $(v_M)_j$  are chosen to be the Petrov-Galerkin weight function on a compact support sub-domain of each node [13]. The weight function of node  $i$  equals unity at  $x_i$ , and monotonically decreases as  $\|x - x_i\|$  increases and is equal to zero at the boundary and outside of the sub-domain.

#### Trial functions in the transition region

The trial functions in the transition region need special attention. Different numerical methods (MM, BEM, and different types of elements of FEM) use distinct trial functions. Directly coupling two numerical methods by only matching the interface nodal values may not satisfy the compatibility condition along the interface. In other words, the function values produced in different regions along the interface may be different although a few nodal values are the same. Therefore, a transition element between the two regions that smoothly transforms the values of the trial functions from one region to another is preferred.

A blending technique is developed to generate the interpolation function in a 4-sided region (quadrilateral element) in terms of its edge (boundary) functions (see Figure 4). The edges of the element can be curved and the number of the nodes on each of the edges need not be the same. This technique is similar to a technique, 'Coons patch' [23], that is used in computer-aided geometric design and FEM mesh generation. The Coons patch technique is used to construct a smooth surface using the bounded curves. By using the Coons patch technique in an analogous fashion, the various trial functions on the edges of the transition elements are blended smoothly. This technique is also similar to the method used to generate serendipity elements. However, instead of using the boundary nodal values to generate the serendipity element, the boundary functions are used in this blending technique to construct the transition element. These boundary functions may be explicit functions of the boundary nodal values, such as FEM, or implicit functions of the nodal values, such as MM.

A bilinear blending is used in this study to construct the trial function of the element. Although the blending is *bilinear*, the trial functions can be an *arbitrary* function that depends on the edge functions of the element [23]. To be compatible with the FE method, the trial functions of the transition element are developed in a square element (parent element) in the ' $\xi, \eta$ ' domain, where  $-1 \leq (\xi, \eta) \leq 1$ . The trial function can be written as

$$\begin{aligned}
 u = & \frac{1}{2}(1-\xi) \cdot \Gamma_3(\eta) + \frac{1}{2}(1+\xi) \cdot \Gamma_4(\eta) \\
 & + \frac{1}{2}(1-\eta) \cdot \Gamma_1(\xi) + \frac{1}{2}(1+\eta) \cdot \Gamma_2(\xi) \\
 & - \frac{1}{4}(1-\xi)(1-\eta) \cdot u_n - \frac{1}{4}(1+\xi)(1-\eta) \cdot u_p \\
 & - \frac{1}{4}(1+\xi)(1+\eta) \cdot u_q - \frac{1}{4}(1-\xi)(1+\eta) \cdot u_m
 \end{aligned} \quad (15)$$

where  $\Gamma_i$  ( $i = 1, 4$ ) are the boundary functions of the quadrilateral element and  $u_j$  ( $j = n, p, q$ , and  $m$ ) are the values of the primary variable at the corner nodes.

The derivatives of the primary variable with respect to  $x$  and  $y$  can be obtained by calculating the derivatives with respect to  $\xi$  and  $\eta$ , then forming the Jacobian matrix of the element and following standard FE procedures.

Typical transition elements between the FE region ( $\Omega_F$ ) and MM region ( $\Omega_M$ ) are shown in Figure 5. The open circles and solid circles represent the nodes in the FE and MM regions, respectively. The shaded elements are the transition elements. In these transition elements, the solid lines represent the boundaries that are connected to finite elements. On these boundaries, the edge functions can be generated by FE trial functions. The dashed lines in Figure 5 are the boundaries that connect to the MM region, and the edge functions are generated by the MM trial functions. The next step is to form the test function for the transition elements.

### Test functions in the transition region

Although the test function can be arbitrarily selected in the weighted residual method, to satisfy the weak form requirement of the reciprocity conditions of the secondary variables with constant derivatives (see Eq. (8)), the test functions  $v$  must (a) be the same function and (b) have the same integration length along the interface of both of the regions. Therefore, the test function of a node in the transition element depends on the adjacent regions of that node. If the node is adjacent only to the FE region, and not to the MM region, the FE test function is used and the integration length of the function is identical to the side of the element (for

example, the side lengths are  $a$  and  $b$  in type C of Figure 5 for node  $g$ ). For a node that connects to the MM region, the MM test function with a support domain of  $l_0$  is used (for example nodes  $q$  and  $k$  of type B in Figure 5).

One additional concern about the test function of the transition region is the size of the support domain of a node using an MM test function. The size of the support domain of an MM node can be defined by a process similar to that used in references [11-14]. Although there is no restriction on the size of the support domain by the weighted residual method, the radius ( $l_0$ ) of the support domain of a node is defined to be less than the size of the element to which that node belongs (see for example, nodes  $q$  and  $k$  of type B in Figure 5). This limitation on the size of the support domain eliminates complicated numerical integration that may be needed to integrate accurately the weak form of the transition element.

In Figure 5, three types of possible transition elements, A, B, and C, are identified. In the type B element, the nodes  $k$  and  $q$  are on the interface  $\Gamma_1$ . Therefore, the MM trial function is applied on edge  $kq$ , and the MM test functions should be applied on both nodes  $k$  and  $q$ . Note the sizes of the support domain ( $l_0$ ) of the test function for nodes  $k$  and  $q$  need not be the same. Since node  $q$  is shared by elements of type A and B, in order to satisfy the reciprocity conditions of the secondary variables on the common edge  $pq$ , the MM test function should be applied on node  $q$  of the element of type A, although no MM trial function is applied on any edge in element of type A.

### System equations

The trial and test functions outlined in Eqs. (10-15) are substituted into the weak form in Eq. (9) and the integrations are performed. This leads to a system of equations similar to the FE and MLPG methods

$$[\mathbf{K}] \cdot \{\mathbf{u}\} = \{\mathbf{f}\} \quad (16)$$

where  $[\mathbf{K}]$  contains the  $[\mathbf{K}_F]$ ,  $[\mathbf{K}_M]$  and  $[\mathbf{K}_T]$  matrices corresponding to the FE, MM and transition regions, respectively. Similarly,  $\{\mathbf{f}\}$  contains contributions from the three regions. The solution of the system of equations leads to the potentials  $\{\mathbf{u}\}$  at all the nodes in the model. Note that instead of working with fictitious nodal potentials  $\{\hat{\mathbf{u}}\}$  in the MM method the nodal potentials  $\{\mathbf{u}\}$  are used by making use of the procedures contained in reference [14].

### Boundary conditions

There are no special considerations necessary to apply essential boundary conditions on the model. However, the values of the natural boundary condition ('force')

depend on the type of nodes (FE or MM) on the transition element. Based on Eq.(4), the 'force' value on a node is calculated as

$$f_j = \int_{\Gamma_j} \left( \frac{\partial u}{\partial x} \cdot n_x + \frac{\partial u}{\partial y} \cdot n_y \right) \cdot v_j \cdot d\Gamma - \int_{\Omega_j} p \cdot v_j \cdot d\Omega \quad (17)$$

where  $v_j$  is the test function of the nodes  $j$ ,  $\Gamma_j$  is the boundary of the test function where the secondary variables, fluxes, are prescribed, and  $\Omega_j$  is the domain of the test function.

The formulation presented above for the coupled method is evaluated by performing patch test problems and by application to problems for which exact solutions are available.

### Numerical Examples

To evaluate the algorithm of coupling FE-MM for potential problems, two example problems governed by Poisson's equation, as shown in Figure 6, are considered. For the numerical integration in the MM domain, 8 and 12 Gauss points are used in the radial and tangential directions, respectively, of the circular support domain. A 3x3 quadrature rule is used for the quadratic elements in the FE region. The Gauss quadrature of a node in the transition element is dependent on the test function of the node. For the node using the MM test function, the same Gauss quadrature is used as in the MM region. A 4x4 quadrature rule is used for the node using the FE test functions.

The potential and its partial derivatives obtained using the coupling method are compared to exact solutions wherever available. The error norm ( $\|e_M\|_2$ ) is used to evaluate the effectiveness of various parameters. This norm is defined as

$$\|e_M\|_2 = \sqrt{\sum_{j=1}^M \{(u_j - u_{exact}) / u_{exact}\}^2} / M \quad (18)$$

where  $M$  is the total number of randomly distributed internal points in the domain at which the numerical solution is evaluated and compared to the exact solution. Note that these internal points are independent points that are randomly generated and are not associated with the nodes used in the models. In the MM region, a value of  $M = 50$  is used, and in the FE region, six randomly distributed points are generated for each element. The error norm is calculated for the entire domain. If the exact solution of the problem is not available, the results of the coupling method are compared to the full FE solutions and the full MM solutions over the analysis domain.

Two types of interfaces are used to model the examples. The first type of interface cuts across the domain and intersects the domain boundary as shown in Figure 2(a).

The second type of interface forms a closed loop and does not intersect the domain boundary (see Figure 2(b)). Two types of models are used to evaluate this type of interface. The first model uses an FE region that is embedded in an MM region, and the second model uses an MM region that is embedded in an FE region.

In the examples (see Figure 6), 8-node quadratic isoparametric elements and quadratic basis functions in the MM region are used. When the coupled method reproduces the exact solution, then the method "passes" the patch tests.

### Example 1

A potential problem governed by the Poisson's equation,  $\nabla u^2 = 2 \cdot (c_1 + c_2)$  is considered in a rectangular domain (Figure 6(a)). The exact solution for the problem is  $u = c_1 x^2 + c_2 y^2 + c_3 xy$ , where  $c_i$  are arbitrary constants. All four models in Figure 7 are used to evaluate the coupling method using quadratic quadrilateral elements and a quadratic basis function in the FE and MM regions, respectively. A type-I interface is used in the first model, and a type-II interface is used in the models 2, 3 and 4. In these patch tests, the potential  $u$  is prescribed on the boundaries of the entire domain corresponding to the exact values. As expected, the exact solutions for both potential and fluxes in the entire domain are reproduced to machine accuracy. Similar results are obtained using the mixed boundary conditions.

### Example 2

The second example considered is that of the torsion of a shaft of elliptical cross-section as shown in Figure 6(b). The governing equation is a Poisson's equation in terms of Prandtl stress function  $u$  with the boundary condition  $u = 0$  on the boundary of the cross-section. The shear stresses in the shaft are determined as the derivatives of the stress function. For this problem, the right-hand side function of Eq. (1) is defined as

$$p(x, y) = -2G\theta = -\frac{2 \cdot M \cdot (a^2 + b^2)}{\pi \cdot a^3 \cdot b^3} \quad (19)$$

where  $G$  is the modulus of rigidity,  $\theta$  is the twist angle,  $M$  is the torsion moment applied on the shaft, and  $a$  and  $b$  are the semi-major and semi-minor axes of the elliptic cross-section, respectively. The exact solution of the problem [24] is

$$u(x, y) = -\frac{M}{\pi \cdot a \cdot b} \left( \frac{x^2}{a^2} + \frac{y^2}{b^2} - 1 \right) \quad (20)$$

Two coupling models are used for the problem, a full model of the elliptic shaft and a model of one-quarter of the shaft, as shown in Figure 8. As the exact solution is a quadratic, quadratic elements and quadratic basis

functions are used. In the full model, 16 quadratic elements (8-node quadrilateral) and 102 MM nodes using a quadratic basis function are used. The essential boundary condition of  $u = 0$  is applied on the outer surface of the elliptic cross-section. In the model of one-quarter of the elliptic shaft, 4 quadratic elements and 38 nodes are used. The essential boundary condition ( $u = 0$ ) is applied on the outer surface and the natural boundary conditions ( $q = 0$ ) are applied on the symmetric centerlines ( $y = 0$  and  $x = 0$ ).

The error norm of the results for the potential and its first derivatives are computed using the exact solution at 100 randomly distributed points in the MM region and 96 random points in the FE region for the whole model. For the model of one-quarter of the elliptic shaft, 50 and 24 points are used in the MM and FE regions, respectively. The exact solutions are reproduced to machine accuracy for both models.

### Concluding Remarks

A technique is presented for coupling the traditional finite element (FE) method and the meshless method (MM) for analyzing two-dimensional potential problems that are governed by Poisson's equation. The coupling method allows the domain to be analyzed by the FE method in one region and the MM in another region. The regions are chosen depending on where each of methods is most effective.

A single variational weighted residual formulation is used on the entire domain to develop the coupling method. A transition region is defined between the FE region and the MM region. In the transition region, a blending technique is used to construct the trial function based on the trial function in the adjacent region. The MM and FE test functions are used in the transition region to satisfy the compatibility condition of the secondary variables.

Potential patch test problems involving Poisson equation are used to evaluate the effectiveness of the coupling technique when the meshless local Petrov-Galerkin method is used in the MM region. The coupling method passed all the patch test problems and yielded very accurate solutions for the problems studied.

### References

- [1] Zienkiewicz, O.C., and Taylor, R.L., *The Finite Element Method*, 4th ed, McGraw-Hill Book Company, 1989.
- [2] Cook, R.D., Malkus, D.S., and Plesha, M.E., *Concepts and Applications of Finite Element Analysis*, 3rd ed, John Wiley and Sons, 1989.
- [3] Nayroles, B., Touzot, G., and Villon, P., "Generalizing the Finite Element Method: Diffuse Approximation and Diffuse Elements," *Computational Mechanics*, Vol. 10, No. 5, 1992, pp. 307-318.
- [4] Belytschko, T., Lu, Y.Y., and Gu, L., "Element-Free Galerkin Methods," *International Journal for Numerical Methods in Engineering*, Vol. 37, No. 2, 1994, pp. 229-256.
- [5] Belytschko, T., Lu, Y.Y., and Gu, L., "Crack Propagation by Element-Free Galerkin Methods," *Engineering Fracture Mechanics*, Vol. 51, No. 2, 1995, pp. 295-315.
- [6] Lu, Y.Y., Belytschko, T., and Gu, L., "New Implementation of the Element Free Galerkin Method," *Computer Methods in Applied Mechanics and Engineering*, Vol. 113, No. 3-4, 1994, pp. 397-414.
- [7] Duarte, C., and Oden, J.T., "Hp Clouds - an Hp Meshless Method," *Numerical Methods for Partial Differential Equations*, Vol. 12, 1996, pp. 673-705.
- [8] Melenk, J.M., and Babuska, I., "The Partition of Unity Finite Element Method: Basic Theory and Applications," *Computer Methods in Applied Mechanics and Engineering*, Vol. 139, 1996, pp. 289-314.
- [9] Liu, W.K., Jun, S., and Zhang, Y.F., "Reproducing Kernel Particle Methods," *International Journal for Numerical Methods in Engineering*, Vol. 20, 1995, pp. 1081-1106.
- [10] Zhu, T., Zhang, J.D., and Atluri, S.N., "A Local Boundary Integral Equation (LBIE) Method in Computational Mechanics, and a Meshless Discretization Approach," *Computational Mechanics*, Vol. 21, No. 3, 1998, pp. 223-235.
- [11] Atluri, S.N., and Zhu, T., "A New Meshless Local Petrov-Galerkin (MLPG) Approach in Computational Mechanics," *Computational Mechanics*, Vol. 22, No. 2, 1998, pp. 117-127.
- [12] Atluri, S.N., and Zhu, T.L., "Meshless Local Petrov-Galerkin (MLPG) Approach for Solving Problems in Elasto-Statics," *Computational Mechanics*, Vol. 25, No. 2, 2000, pp. 169-179.
- [13] Raju, I.S., and Chen, T., "Meshless Petrov-Galerkin Method Applied to Axisymmetric Problems," *Proceedings of the 42nd AIAA/ASME/ASCE/AHS/ASC Structures, Structural Dynamics, and Materials Conference*, Seattle, Washington, April 16-19, 2001.

- [14] Atluri, S.N., Kim, H.-G., and Cho, J.Y., "A Critical Assessment of the Truly Meshless Local Petrov-Galerkin (MLPG), and Local Boundary Integral Equation (LBIE) Methods," *Computational Mechanics*, Vol. 24, No. 5, 1999, pp. 348-372.
- [15] Zienkiewicz, O.C., Kelly, D.W., and Bettress, F., "The Coupling of the Finite Element Method and Boundary Solution Procedures," *International Journal for Numerical Methods in Engineering*, Vol. 11, 1977, pp. 355-375.
- [16] Krishnamurthy, T., and Raju, I.S., "Coupling Finite and Boundary Element Methods for Two-Dimensional Potential Problems," *International Journal for Numerical Methods in Engineering*, Vol. 36, 1993, pp. 3593-3616.
- [17] Belytschko, T., Organ, D., and Krongauz, Y., "Coupled Finite Element-Element-Free Galerkin Method," *Computational Mechanics*, Vol. 17, No. 3, 1995, pp. 186-195.
- [18] Liu, G.R., and Gu, Y.T., "Coupling of Element Free Galerkin and Hybrid Boundary Element Methods Using Modified Variational Formulation," *Computational Mechanics*, Vol. 26, No. 2, 2000, pp. 166-173.
- [19] Liu, G.R., and Gu, Y.T., "Meshless Local Petrov-Galerkin (MLPG) Method in Combination with Finite Element and Boundary Element Approaches," *Computational Mechanics*, Vol. 26, No. 6, 2000, pp. 536-546.
- [20] Hegen, D., "Element-Free Galerkin Methods in Combination with Finite Element Approaches," *Computer Methods in Applied Mechanics and Engineering*, Vol. 135, No. 1-2, 1996, pp. 143-166.
- [21] Huerta, A., and Fernandez-Mendez, S., "Enrichment and Coupling of the Finite Element and Meshless Methods," *International Journal for Numerical Methods in Engineering*, Vol. 48, No. 11, 2000, pp. 1615-1636.
- [22] Rao, B.N., and Rahman, S., "A Coupled Meshless-Finite Element Method for Fracture Analysis of Cracks," *International Journal of Pressure Vessels and Piping*, Vol. 78, No. 9, 2001, pp. 647-657.
- [23] Coons, S.A., "Surfaces for Computer-Aided Design of Space Forms," MIT, MAC - TR - 41, Cambridge, Mass., 1967.
- [24] Timoshenko, S.P., and Goodier, J.N., *Theory of Elasticity*, 3rd ed, McGraw-Hill, New York, 1965.

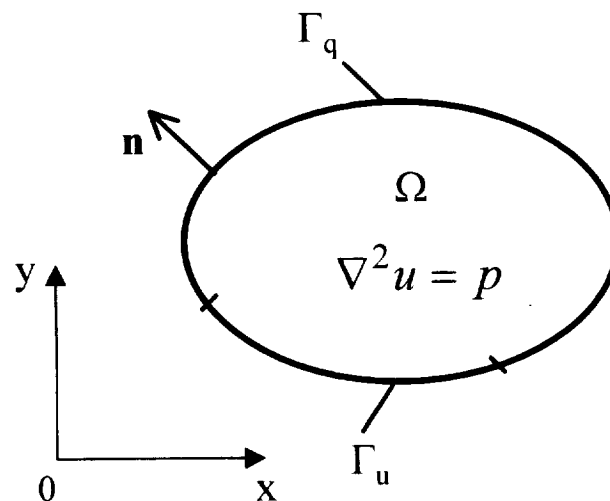


**Figure 1** Two-dimensional potential problem

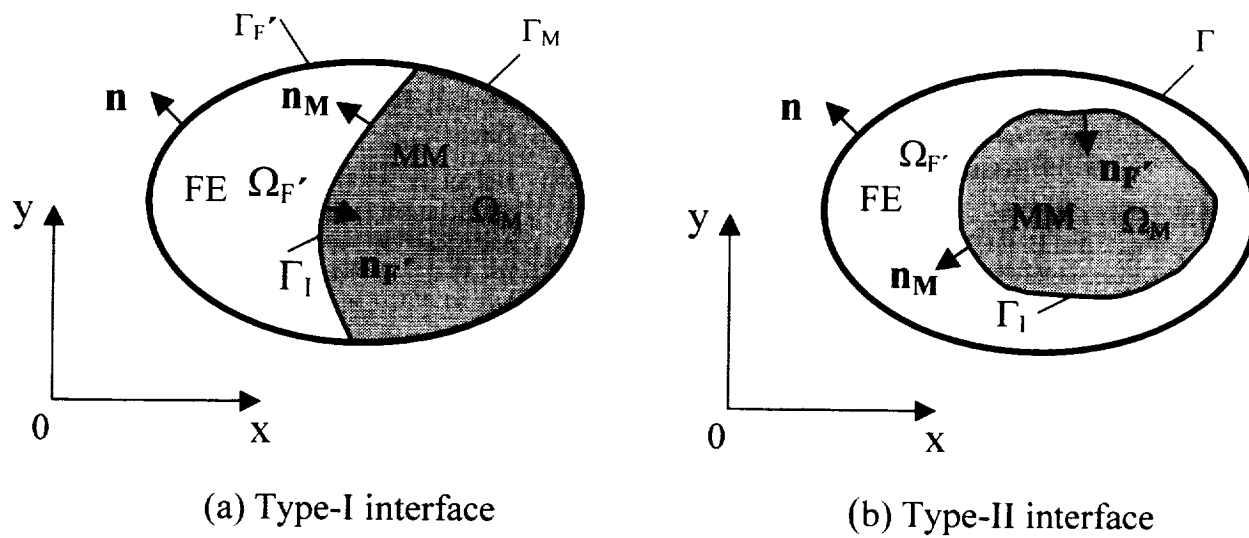


**Figure 2** Finite element and meshless method regions

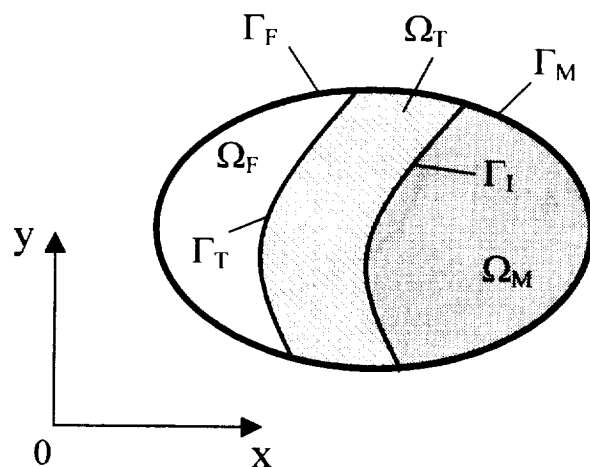


**Figure 3** Finite element (FE) region, transition (TR) region and meshless method (MM) region



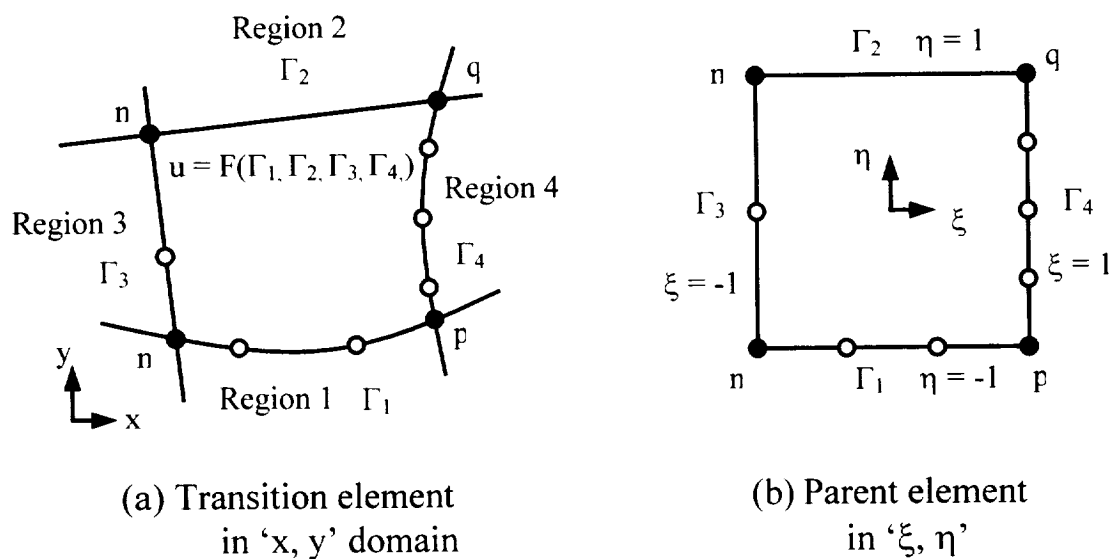


**Figure 4** Construction of transition element

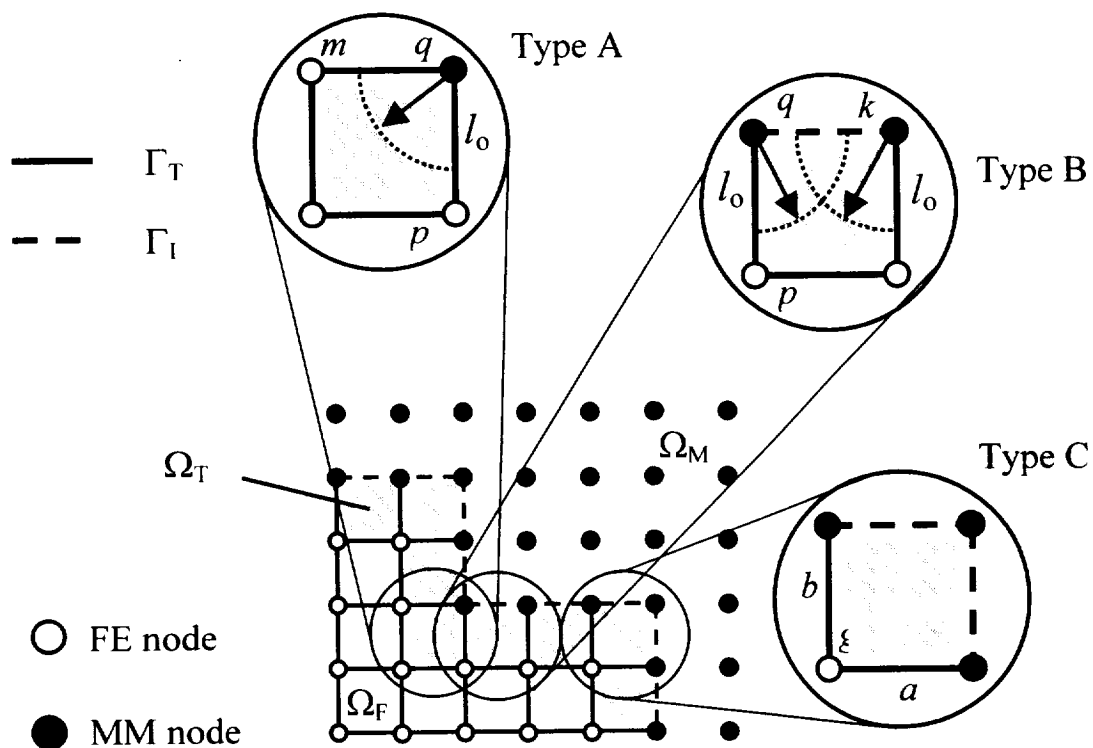
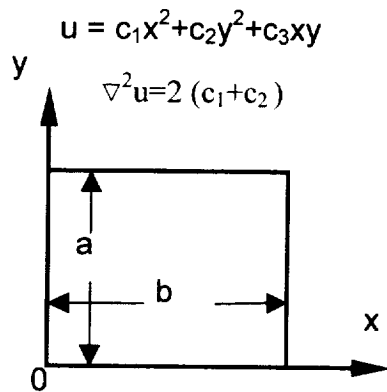
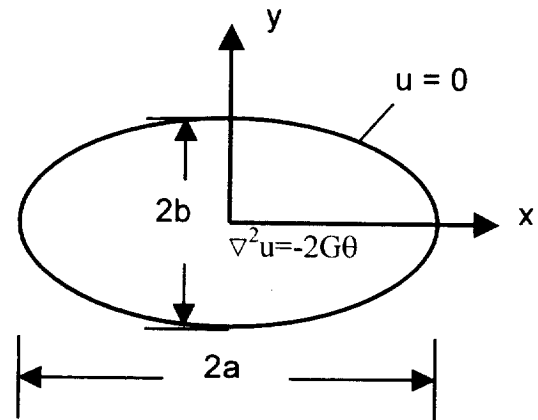


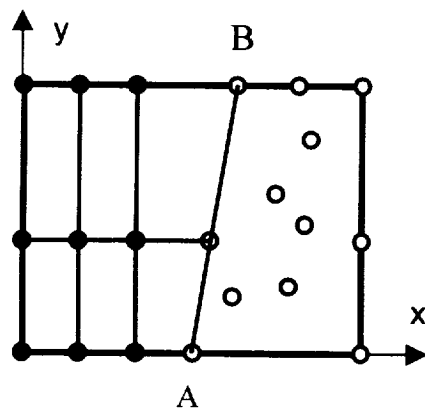
**Figure 5** Typical transition elements



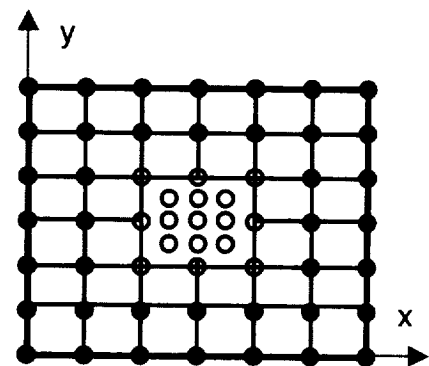
(a) Example - 1



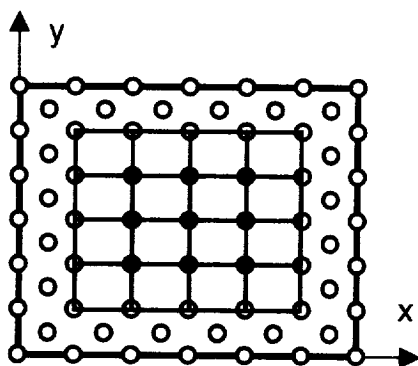
(b) Example - 2

**Figure 6** Examples governed by Poisson's equation

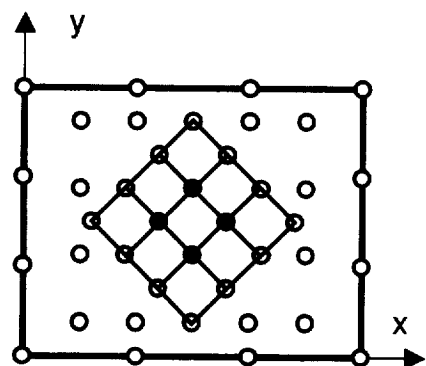
(a) Model 1



(b) Model 2

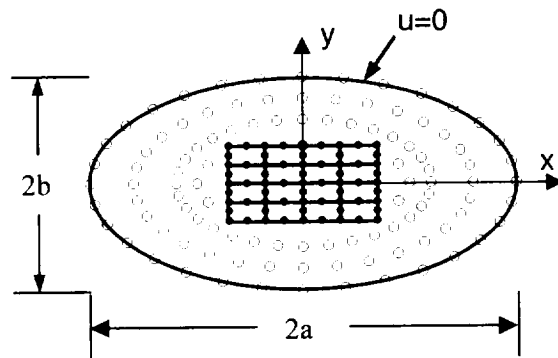


(c) Model 3

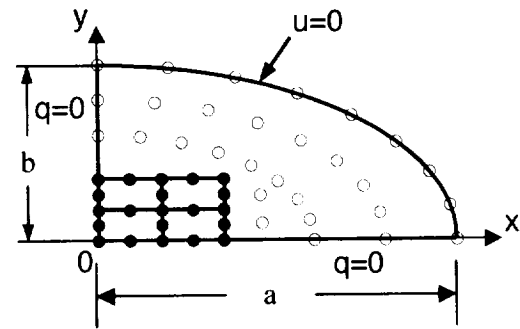


(d) Model 4

**Figure 7** Models used in the patch tests



(a) Whole elliptic shaft model



(b) Model of one-quarter of elliptic shaft

**Figure 8** Coupling models used in the elliptic shaft in torsion

